Figure 3.1.6 Correlation Between the Initial Deactivation of the Methanol Catalyst and the Activity of Dehydration Catalysts

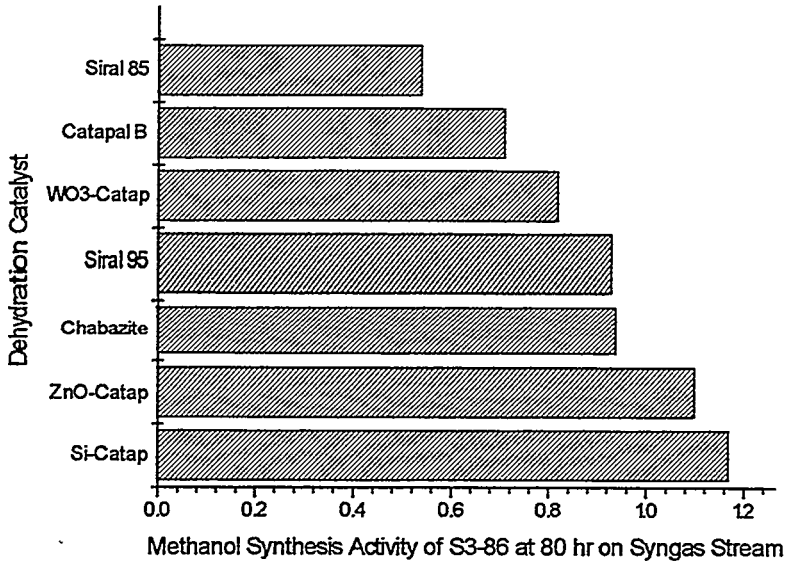

c. Patterns in the Deactivation of Dehydration Catalysts

There are several different patterns in the deactivation of different dehydration catalysts. The first pattern includes MgY, Chabazite, Siral 85, and WO_3-Catapal. This group of catalysts is characterized by rapid initial deactivation to a small residual activity. Significant deactivation occurs during reduction. For example, although Siral 85 has a known higher dehydration activity than g-alumina, its measured initial activity is much lower than that of Catapal B (1.2 vs. 17 mol/kg-hr, see Fig. 3.1.4). The Chabazite and MgY samples were expected to have activities comparable to g-alumina, but their measured initial activities were much lower than expected (Fig. 3.1.4). This rapid deactivation continued when the system was switched to syngas, and the dehydration activity dropped to a residual level within 100 hr on syngas stream.

Si-modified Catapal B g-alumina represents another extreme. No significant initial deactivation was observed. Instead, there was only a slow, long-term deactivation (Fig. 3.1.2).

Catapal B g-alumina undergoes a two-stage deactivation: an initial rapid deactivation (~ 40% loss in its activity) followed by a slower but continuous deactivation. ZnO-modified Catapal also falls into this pattern.

The rapid initial deactivation of dehydration catalysts may depend on the type as well as the strength of acid sites on the catalysts. MgY and Chabazite are typical Bronsted acids. Their fast deactivation may be indicative of the extra vulnerability of the Bronsted acid under LPDME conditions. Siral 85 and Catapal B should contain both Bronsted and Lewis acid sites according to conventional knowledge. Without solid evidence, it is assumed for the time being that the fast deactivation of Siral 85 and of Catapal B in the initial stage is due to the acid sites of great strength and/or Bronsted nature. This assumption is supported by the following observation.

The initial fast deactivation of Catapal B can be eliminated by modifying the surface with silica (Si-modified Catapal B), a process called silylation, and known for eliminating strong and Bronsted acid sites. It may not be just a coincidence that this passivated catalyst starts with an activity similar to that of the virgin Catapal B alumina after the first stage of deactivation.

The long-term deactivation of dehydration catalysts does not follow any clear pattern. The deactivation varies from one system to another. The higher dehydration activity (i.e., greater acidity) does not necessarily result in faster deactivation of the dehydration catalyst, or vice versa. This is clearly illustrated by the results from the Si- and WO_3-modified Catapal B samples shown in Figure 3.1.2.

d. Deactivation of the Methanol Catalyst vs. That of Dehydration Catalysts

In the standard catalyst system the initial deactivation of the methanol catalyst is accompanied by a corresponding deactivation of Catapal B alumina (Figs. 3.1.1 and 3.1.2). Relatively stable Si-Catapal B and ZnO-Catapal B correspond to smaller initial deactivation of the methanol catalyst. However, the almost complete deactivation of Chabazite and MgY samples is not accompanied by significant initial deactivation of the methanol catalyst (Figs. 3.1.3 and 3.1.4). And the initial loss in the methanol activity is totally outweighed by that of the dehydration activity in the case of Siral 85.

This lack of correlation between the deactivation of the methanol catalyst and the deactivation of dehydration catalysts can be further illustrated. Figures 3.1.7A and 3.1.7B plot the ratio of the methanol synthesis rate constant to the dehydration rate constant, both normalized by their initial values, for different catalyst systems. This serves as a measurement of the relative deactivation rates of two catalysts in a given catalyst system. It can be seen that the ratio is about 1 for the standard catalyst system, the systems containing silica alumina (Siral 85 and 95), and ZnO-modified Catapal B. In the case of Si-modified Catapal, the dehydration catalyst deactivates more slowly than the methanol catalyst. For the rest of the catalyst systems, the dehydration catalyst deactivates much faster than the methanol catalyst. This variation suggests that the deactivation of methanol and dehydration catalysts does not have to be a concerted process. Furthermore, different deactivation mechanisms may be operational for different catalyst systems.

Figure 3.1.7A The Deactivation Rate of the Methanol Catalyst Relative to that of Dehydration Catalysts in Different Catalyst Systems

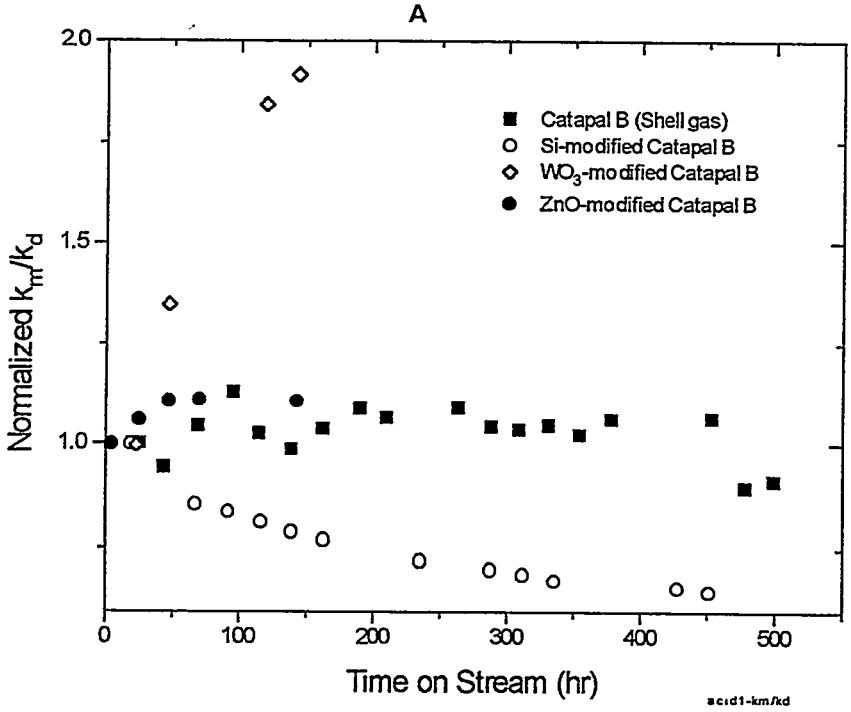

Figure 3.1.7B The Deactivation Rate of the Methanol Catalyst Relative to that of Dehydration Catalysts in Different Catalyst Systems

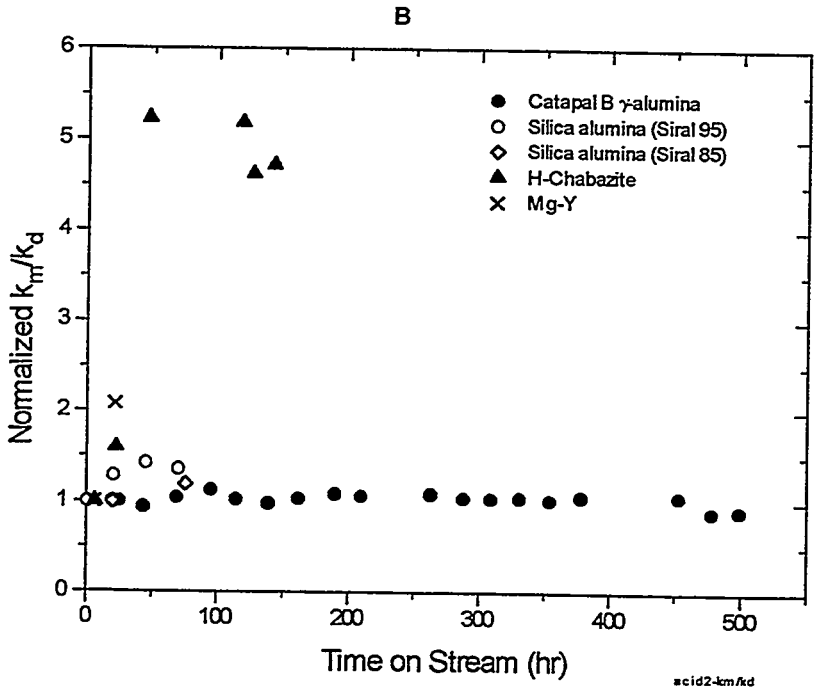

e. Mechanistic Considerations

The initial deactivation of the methanol catalyst is possibly *driven by the acid-base interaction* between the two catalysts, since it correlates with the dehydration activity (Fig. 3.1.6). Among the possible mechanisms are the inter-catalyst mass transfer and inter-catalyst solid state reaction. For instance, ion exchange could take place between Cu- and Zn-containing species from the methanol catalyst and the protons on the dehydration catalyst. Or the deactivation could be due to a reaction between ZnO (a base) in the methanol catalyst and the acid sites on a dehydration catalyst. The same acid-base interaction may also be responsible for the initial deactivation of dehydration catalysts.

Surprisingly, the initial deactivation of the methanol catalyst is not correlated to the initial deactivation of dehydration catalysts, considering that both may be due to the acid-base interaction. However, this lack of correlation can be understood if acid sites of different natures (Bronsted or Lewis) undergo deactivation through different routes. Furthermore, we still have not ruled out the possibility that coke formation deactivates, as a parallel route, dehydration catalysts. If it is, certainly it will complicate the pattern of the deactivation of dehydration catalysts.

The mechanism for the long-term deactivation of both methanol and dehydration catalysts is not clear. For one thing, it is not directly related to the dehydration activity. The long-term deactivation may still be due to inter-catalyst mass transfer or solid state reactions, but is not likely acid-base in nature. For example, the migration of Zn- and Cu-containing species from the methanol catalyst to dehydration catalysts can be *driven by the concentration gradient* of these species between the methanol catalyst and dehydration catalysts. Note that most of the metal oxides tested as dehydration catalysts are also good catalyst supports with dispersing capability for metal, metal oxides, and salts, and the dispersing capability is not necessarily related to the acidity of the materials.

3.1.2 What We Learned from the Experiments using Robinson-Mahoney Basket Internals

3.1.2.1 A Repeated Run Using Robinson-Mahoney Basket Internals

A second LPDME run using Robinson-Mahoney (R-M) basket internals was conducted this quarter. The goal of this experiment was twofold: first, to confirm the results from the first experiment using the basket internals because of their important implication for future work, and second, to determine when the deactivation of the dehydration catalyst occurs under this setup.

The current run (14045-69) was carried out at the same conditions as the first one (Shell gas, 750 psig, 250°C). Two different space velocities and stirrer speeds were used in the previous R-M run: 6,000 GHSV and 1600 rpm vs. 1500 GHSV and 2000 rpm. The second set of conditions was used in the current run, which was also shorter, 121 hr compared to 500 hr for the earlier run. As for the first experiment, due to the mass transfer limitations under the R-M setup, the activity of the catalysts could only be checked in a subsequent run using the normal LPDME setup and the powdered catalyst mixture made from the spent pellets. The previous experiment showed that the powders from the R-M experiment were reduced (i.e., hydrogen uptake of the

powder was minimal). Therefore, the system was brought to the reaction conditions without reduction in the run of activity measurement.

Table 3.1.1 lists the activity results of the catalysts from both R-M runs, along with those from a standard LPDME life run (powder mixture, 11782-3). There are some differences between the two R-M runs; mainly, the second run exhibits higher methanol activity and lower dehydration activity. This difference is likely due to the experimental variability. As mentioned previously, the spent pellets were ground into powders, then reloaded into the autoclave to check activity. In both runs, only a portion (1/4 in the first and 1/2 in the second run) of the catalyst mixture was ground, saving the other portion for analytical purposes. Since the pellet mixture might not have been perfectly mixed, the ratio of the two catalysts in the ground samples may have been different from the nominal values, resulting in the uncertainty in data analysis.

Given the experimental variability, the same conclusion can be drawn from the two R-M runs. Judging by the rate constant, the spent methanol catalysts from the R-M runs have almost the same activity as the fresh methanol catalyst in the standard run, and much higher activity than the methanol catalyst at a similar time on stream in the standard run. Therefore, both runs indicate that the methanol catalyst is stable under the R-M setup. The dehydration catalyst deactivated in the R-M runs by 37-59%. Since the longer time on stream in the initial experiment did not result in greater deactivation in the dehydration activity, it can be concluded that the deactivation of the dehydration catalyst occurred only in the earlier stage of the run (< 127 hr). That is, there is no long-term deactivation of the dehydration catalyst under the R-M setup.

Table 3.1.1 Activity of the Catalysts Used in the LPDME Runs Using Robinson-Mahoney Basket Internals

Reaction conditions: 250°C, 750 psig, Shell gas.

Run	Catalyst	Time On-Stream	MEOH Equiv. Prod.	Concentration (%)		Rate Constant	
	S3-86:A1203	(hr)	(mol/kg-hr)	MEOH	DME	k_m[a]	k_d[b]
1st R-M (14045-52)	82.2:17.8	508	28.1	1.59	6.13	2.7	10.7
2nd R-M (14045-75)	**80:20**	**127**	**27.1**	**2.74**	**4.87**	**3.1**	**7.0**
Standard (11782-3)	81.3:18.7	20	30.7	1.01	6.95	3.0	17.0
		115	23.6	0.83	4.89	19	10.8
		499	30.37	0.49	2.67	1.0	5.9

a: Methanol synthesis rate constant calculated from $R_m = k_m f_{H_2}^{2/3} f_{CO}^{1/3}$ (1-*appr.*), based on methanol catalyst weight.

b: ethanol dehydration rate constant calculated from $R_d = k_d f_{CO_2}^{-0.33} f_{MEOH}^{0.11} f_{CO}^{0.70}$ (1-*appr.*), based on alumina weight.

3.1.2.2 The Role of Intimate Contact Between the Two Catalysts in Catalyst Deactivation

There are two important observations from the experiments using Robinson-Mahoney basket internals and pelletized catalysts. First, this system is free of methanol catalyst deactivation,

indicating that the presence of an active dehydration catalyst in the system does not necessarily cause the deactivation of the methanol catalyst. This is true for even the potential initial deactivation stage, a stage associated with dehydration activity. It also indicates that the slurry fluid does not participate in deactivation of the methanol catalyst.

Second, we did see initial deactivation of the dehydration catalyst under this setup. This deactivation may be due to either inter-catalyst mass transfer or coking. The analysis of the spent samples from this experiment will enable us to distinguish between these two mechanisms. If inter-catalyst mass transfer is the cause, the slurry fluid must have served as the mass transfer medium. And apparently the methanol catalyst has some "free" Zn- and/or Cu-containing species to spare before its activity starts to suffer. *In summary, among four modes of catalyst deactivation under the standard LPDME conditions, three of them do not occur under the Robinson-Mahoney setup.*

Why is the catalyst deactivation pattern so different between a normal slurry phase operation and the run using Robinson-Mahoney basket internals and pelletized catalysts? If one assumes that the inter-catalyst mass transfer or reaction causes the deactivation of both catalysts, this process requires a **driving force** and the **intimate contact** between two catalysts. The driving force, as discussed above, could be acid-base interaction between the methanol catalyst and dehydration catalysts (the initial deactivation of both catalysts), or simply the concentration gradient between the two catalysts and the dispersion capability of dehydration catalysts (the long-term deactivation of both catalysts). The driving force alone is not sufficient; intimate contact between the two catalysts is necessary to provide the time and area for the mass transfer or/and reaction to take place.

One can envision that the solid state reaction between the two catalysts can only occur when they touch each other and remain that way for a long enough time. Under the slurry phase operation conditions, this intimate contact can be provided by: 1) collision between the catalyst particles, 2) the attachment of small particles to the large ones, either on the outside surface or inside the pores, and 3) the agglomeration of small particles. Collision and attrition continuously generate particles of smaller and smaller size, resulting in large and fresh (therefore active) contact area.

3.1.3 Efforts in Developing Stable LPDME Catalysts

According to the above analysis, the stability of LPDME catalyst systems should be improved by eliminating or reducing either the driving force for the inter-catalyst mass transfer/reaction or the intimate physical contact between the two catalysts. In principle, these can be accomplished by using:

- Chemically modified alumina or methanol catalysts to reduce the driving force of the interaction between methanol and dehydration catalysts, such as removal of strong acid sites.

- Physically modified alumina or slurry system to eliminate the contact between the two catalysts.

- Alternative methanol catalysts such as one-component catalyst systems.

The following are the efforts we have made in these directions this past quarter.

3.1.3.1 Improvement in the Long-Term Stability of the Methanol Catalyst using K-Doped Alumina

A potassium-doped Catapal B g-alumina sample was prepared by impregnating Catapal B g-alumina with a KOH solution. This catalyst was used in a LPDME run along with S3-86 methanol catalyst (19045-85). As shown in Figure 3.1.8, the stability of this catalyst system is better than the standard system (S3-86 plus virgin Catapal B g-alumina). However, its productivity is lower due to the low dehydration activity of the K-doped alumina (Figure 3.1.9). This low activity apparently is due to the high K loading.

Figure 3.1.8 Productivity as a Function of Time

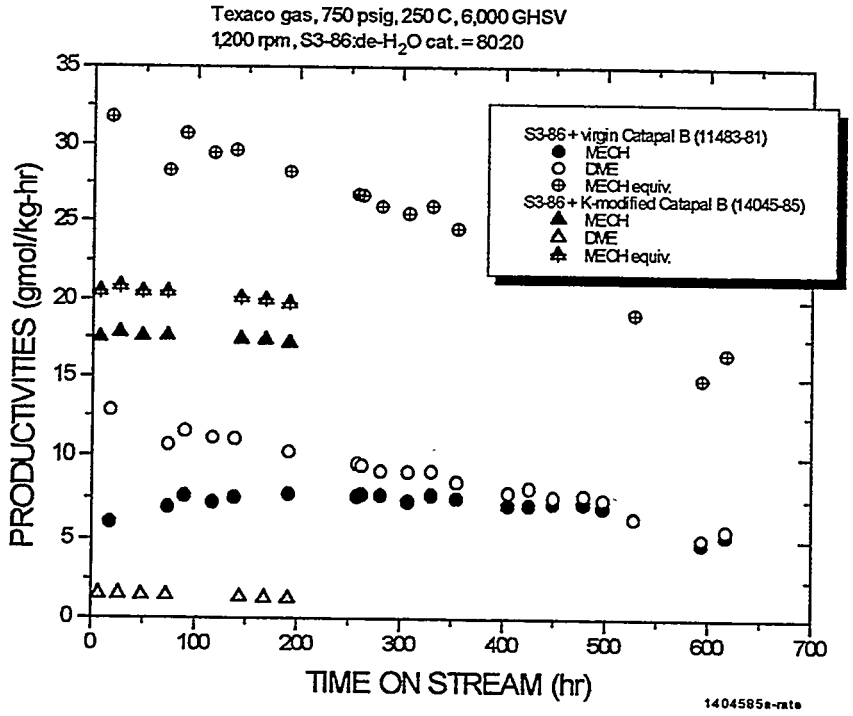

Figure 3.1.9 Dehydration Rate Constants of Different Catalyst Systems as a Function of Time

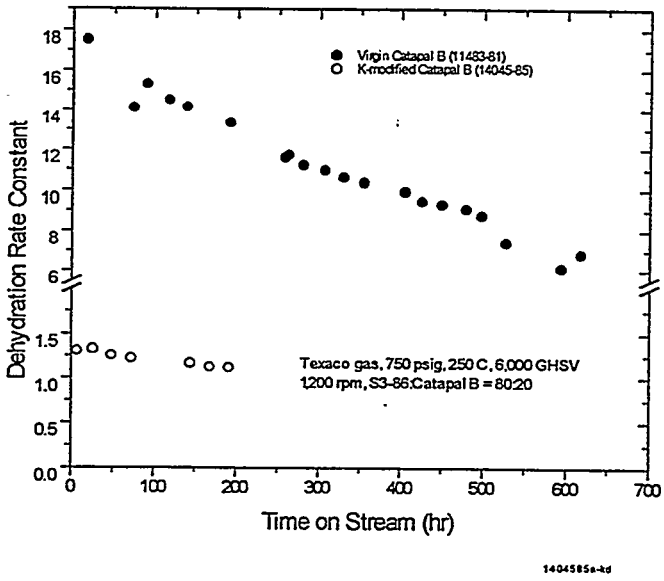

An important observation from this experiment is the improved stability of the methanol catalyst. As shown in Figure 3.1.10, the methanol catalyst has a higher initial activity (i.e., smaller initial deactivation) and slower long-term deactivation, compared to the standard system. Smaller initial deactivation of the methanol catalyst was observed previously whenever a dehydration catalyst without strong acidic sites was used. *However, this is the first time that improvement in the **long-term** stability of the methanol catalyst has been observed.* This improvement cannot be simply attributed to the low dehydration activity of the K-doped alumina. For example, H-Chabazite, Mg-Y, and two silica alumina catalysts (Siral 85 and 95) have a similar or lower dehydration activity than the K-doped alumina upon initial deactivation. However, little improvement in the long-term stability of the methanol catalyst was observed in these systems (Figs. 3.1.3 and 3.1.4).

We have tried to increase the productivity of the current catalyst system by adding more K-doped alumina into the system (from a ratio of 20:80 to 43:57). The productivity is still too low to be attractive. In the coming quarter K-doped alumina samples with lower loading, therefore, higher dehydration activity, will be tested to see if a similar stability can still be obtained.

Another observation from this experiment is that the production of high alcohols, e.g., isobutanol, from this catalyst system is not any higher than a typical LPMEOH run. This suggests that there is little migration of K from the K-doped alumina to the methanol catalyst.

Figure 3.1.10 Methanol Rate Constants of Different Catalyst Systems as a Function of Time

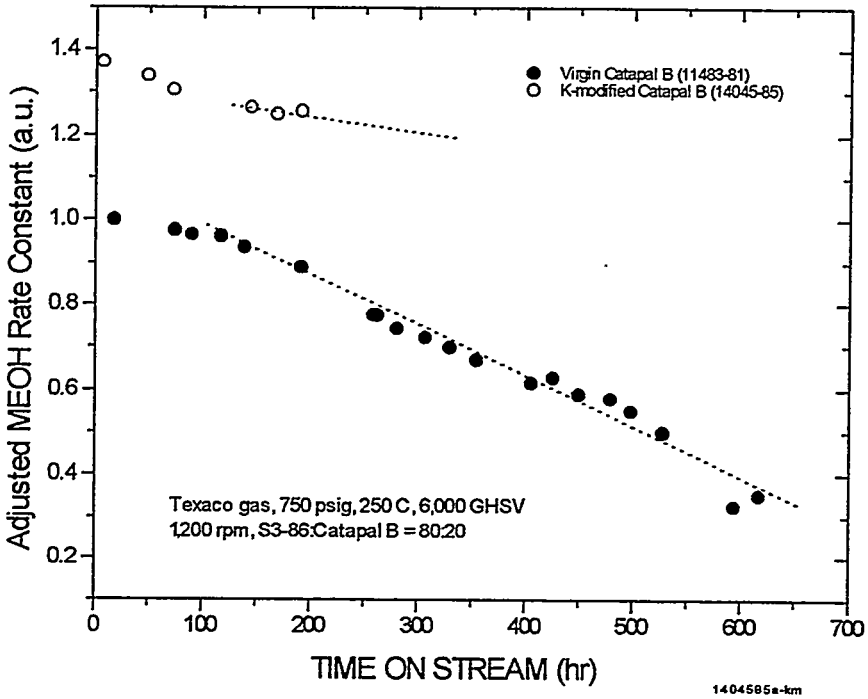

3.1.3.2 Efforts in Passivating the Exterior of Catapal B g-Alumina Particles

A Si-modified Catapal B g-alumina (14191-104) was prepared using a polymeric siloxane precursor. Because of their large size, the siloxane molecules will most likely attach to the outer surface of the alumina. Therefore, when the siloxane is converted into silica upon calcination, only the outer surface of the alumina will be modified or passivated. (This is a technique mentioned in the literature to passivate the strong acid sites on the exterior of zeolites.) Only the outer surface of the alumina is concerned here, because that is where the deactivation of the methanol and dehydration catalysts probably occurs.

Figures 3.1.11a and b display the results of a LPDME run using sample 14045-77, along with samples of a virgin Catapal B g-alumina (14045-63). It can be seen that silica modification of the outer alumina surface results in smaller initial deactivation of the methanol catalyst, as indicated by the greater rate constant for the modified sample compared to that of the unmodified sample (Fig. 3.1.11a). This agrees with our theory that the initial deactivation of the methanol catalyst is due to the strong acid sites on the dehydration catalyst. Figure 3.1.11a shows that the long-term deactivation of the methanol catalyst is also improved somewhat.

Figure 3.1.11b shows that the initial dehydration rate constant of the Si-modified sample is smaller than that of the virgin Catapal B g-alumina, apparently due to reduction in the number of acid sites by the passivation. The modified alumina, however, deactivates more slowly than the virgin one, and becomes more active after 100 hr on stream. In brief, the modification results in significant improvement in the stability of the catalyst system, but not enough as far as the long-term stability of the system is concerned.

Figure 3.1.11 Stability of LPDME Catalyst Systems: Si-Modified vs. Virgin Catapal B

a

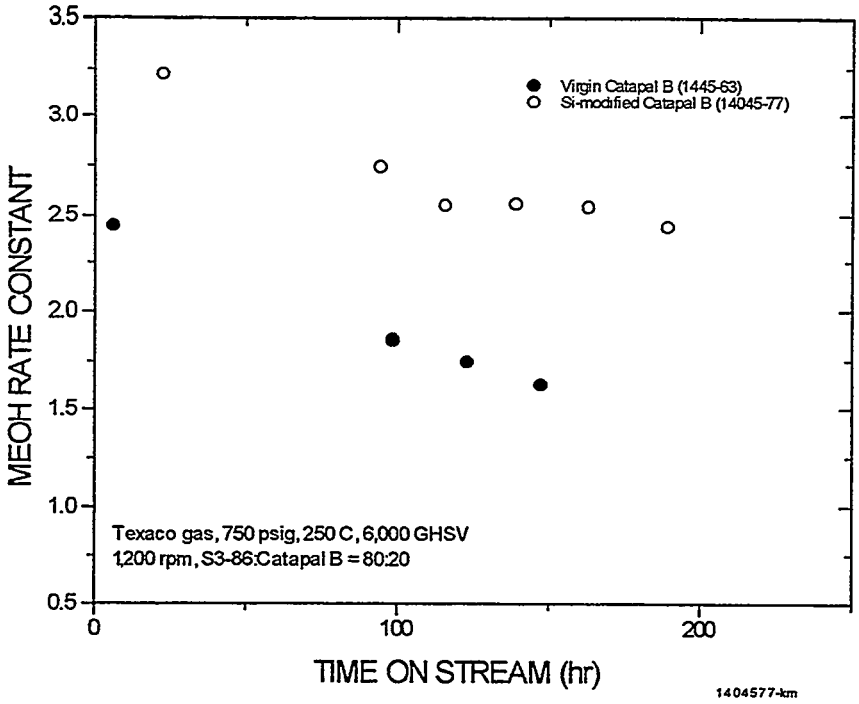

b

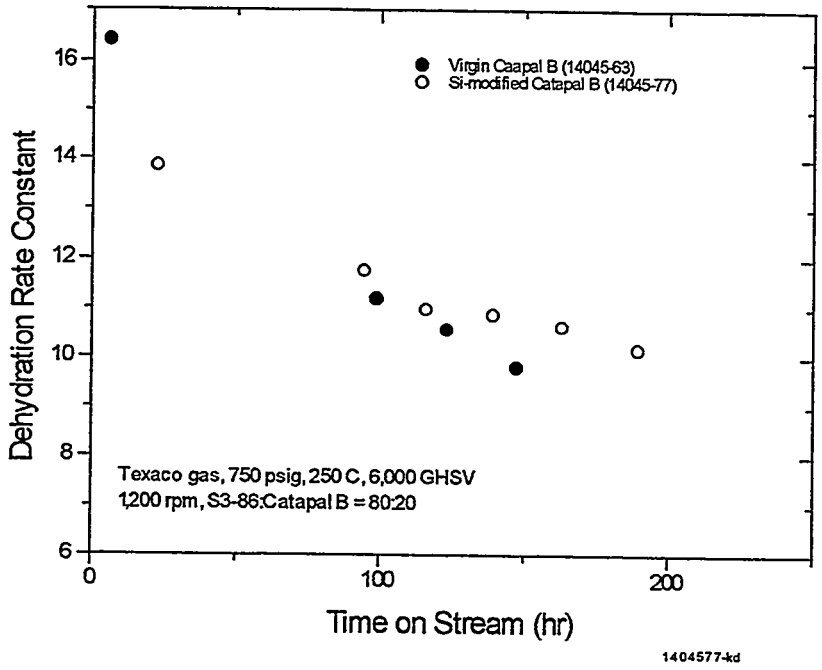

A second sample was prepared in a similar manner, but with much higher Si loading (35 wt % SiO_2). High loading was used so that alumina particles would not be only passivated on the outside surface, but hopefully encapsulated or embedded inside SiO_2. This in turn might reduce the contact between the methanol catalyst and alumina, therefore, improving the stability of the catalyst system. The sample was tested along with S3-86 methanol catalyst at the standard conditions using Texaco gas (14656-17). The dehydration activity of the sample was fairly low, about 19% of the activity of the virgin Catapal B g-alumina. No improvement in the long-term stability of the methanol catalyst was observed from this catalyst system. Note that the technique used in the preparation of this sample is best suited for silylation, but not for encapsulation and embedment.

3.1.3.3 A Single Particle DME Catalyst

A single particle DME catalyst was prepared by impregnating Catapal B g-alumina with zinc and copper (14656-9). The preparation was based on a Shell patent (US 4,375,424, 1983) for a syngas-to-DME catalyst. The catalyst is claimed to perform both methanol synthesis and dehydration functions, and is therefore referred to as single particle catalyst to distinguish it from the dual catalyst mixture in our standard LPDME system.

The standard liquid phase reduction procedure was used to activate this catalyst using 2% H_2 in N_2. The activity of this catalyst was checked using Texaco syngas and standard reaction conditions (250°C, 750 psig, and 6,000 GHSV, run 14045-91). The methanol productivity of this catalyst was found to be an order of magnitude lower than that of our standard dual catalyst system (S3-86 plus Catapal B g-alumina). It is not straightforward to compare this catalyst with the ones reported in Shell's patent, because their test reaction was run at 280°C and 1700 psig. However, catalyst stability is that which is of greatest concern. Figure 3.1.12 depicts the normalized methanol equivalent productivity of this catalyst in comparison with that of our standard dual catalyst system. It can be seen that the rate of deactivation of this one component catalyst is greater than that of our standard dual catalyst system. In the coming months, other one-component catalysts will be examined.

Figure 3.1.12 Stability of the Cu and Zn Doped Alumina Catalyst

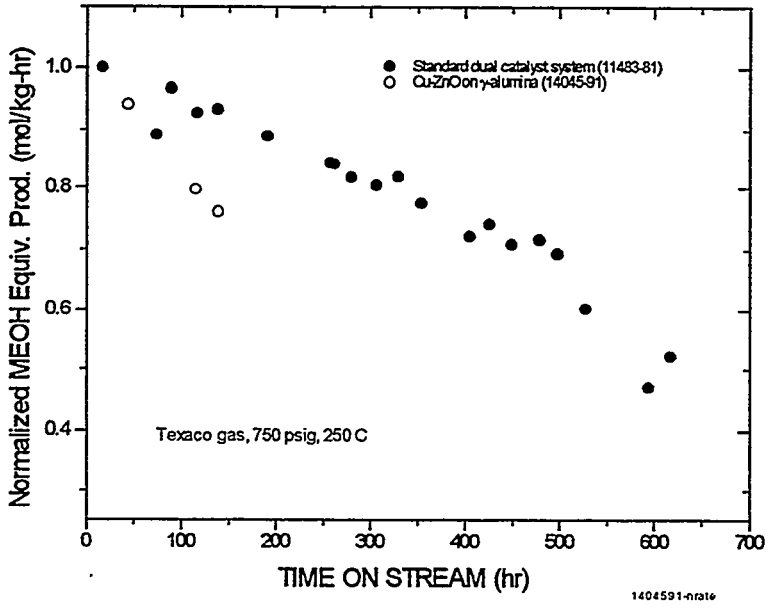

Appendix 3.1.1 The Scheme for Quantification of Catalyst Deactivation

Quantitative description of catalyst deactivation calls for good kinetic models, which are currently not available. What is available are two power law rate expressions as shown below:

$$R_m = k_m f_{H_2}^{2/3} f_{CO}^{1/3} \text{ (1-appr.)} \quad (1)$$

$$R_d = k_d f_{CO_2}^{-0.33} f_{MEOH}^{0.11} f_{CO}^{0.70} \text{ (1-appr.)} \quad (2)$$

where Eq. (1) is the methanol synthesis reaction, Eq. (2) is the methanol dehydration reaction, and *appr.* denotes approach to equilibrium. Both rate expressions have been examined previously (Quarterly Report, April-June 1994). Although both of them have limitations as shown below, they can be used as a semi-quantitative tool to provide the correct ranking in activity among different catalyst systems.

The rate expression for methanol synthesis (Eq. 1) correlates the data from LPDME runs fairly well (14.4% of relative mean deviation in the rate constant, k_m), especially for Shell and Texaco gas under the standard conditions (250°C, 750 psig, 6,000 GHSV), because most of the data used in the regression were obtained in the vicinity of these conditions. However, this rate expression yields rate constants of smaller values when the reaction conditions shift from LPDME to LPMEOH. Figure 3.1.13 illustrates this change as a function of the deviation from the LPDME conditions in terms of DME productivity (RDME). All the data are from freshly reduced catalyst systems (S3-86 plus Catapal B g-alumina, < 25 hr on stream). The variation in DME productivity was achieved by using different ratios of methanol to dehydration catalyst. Equation (1) plus the plots in Figure 3.1.13 provide a scheme to compare the methanol catalyst activity in any catalyst system (S3-86 plus a dehydration catalyst) with that in the standard catalyst system (S3-86 plus virgin Catapal B). That is, the methanol synthesis rate constant of a catalyst system, k_m, is calculated from Eq. (1). This rate constant can then be compared with k_m of the standard catalyst system at a similar dehydration activity (RDME) using Figure 3.1.13. In other words, if we normalize k_m from any catalyst system with that obtained from Figure 3.1.13, we can rank, on a semi-quantitative but consistent basis, the activity of the methanol catalyst in different catalyst systems.

Equation (2) correlates the dehydration data of the standard catalyst system around the standard conditions (250°C, 750 psig, 6,000 GHSV, Shell and Texaco gas) reasonably well (14.1% relative mean deviation in rate constant, k_d). However, poor correlations are observed when the reaction conditions deviate from the standard ones. In addition, there is no reason to believe that the rate expression obtained from Catapal B data should be applicable to other dehydration catalysts. In the absence of a better and universal kinetic model, the rate constant, k_d, from Eq. (2) is used to measure the activity of different dehydration catalysts in the above analysis. Hopefully, Eq. (2) gives us a semi-quantitative description of the activity of dehydration catalysts, that is, the right ranking among different catalysts.

Figure 3.1.13 Adjustment of the Methanol Synthesis Rate Constant as a Function of DME Productivity

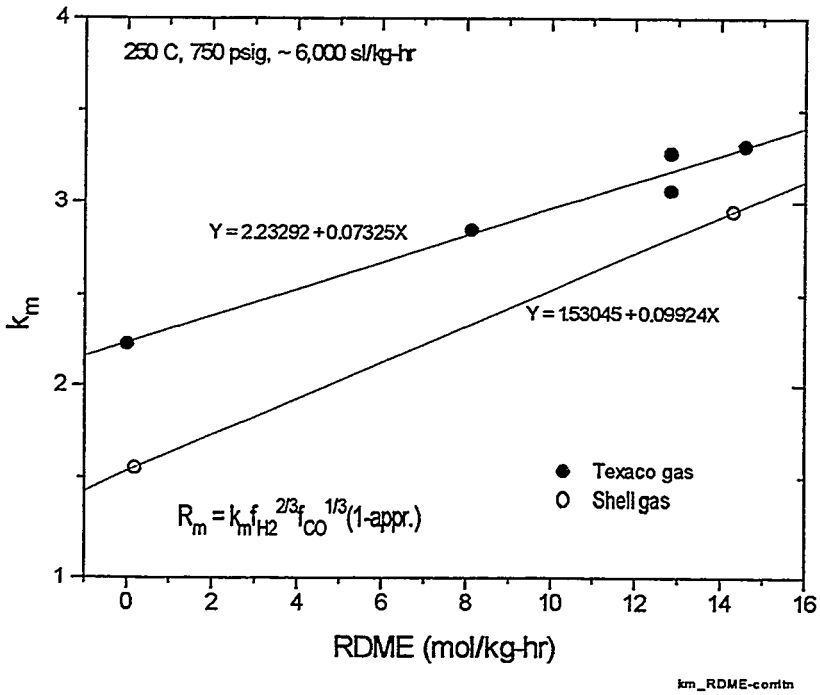

3.2 New Fuels from Dimethyl Ether (DME)

3.2.1 Overall 3 QFY95 Objectives

The following set of objectives appeared in Section III of the previous Quarterly Technical Progress Report No. 2:

- Continue to screen immobilized catalyst candidates for hydrocarbonylation of dimethyl ether to ethylidene diacetate.
- Determine the extent of any catalyst leaching from the best candidate.
- Initiate catalyst development on the cracking of ethylidene diacetate to vinyl acetate and acetic acid.

3.2.2 Chemistry and Catalyst Development

Dimethyl Ether to Ethylidene Diacetate (EDA)

The effort has focused on understanding the rhodium complexes anchored to the Reillex polymers for the catalytic conversion of DME to EDA. The goals were as follows:

- To compare catalytic runs where twice the amount of Reillex was used.
- To compare catalytic runs with different concentrations of rhodium.

- To perform three runs with the same catalyst to investigate loss in activity.
- To investigate the activity of a bimetallic Rh Pd on Reillex.

Catalytic Runs (45 minutes, 300 cc autoclave)
Experiment A
This catalytic run used 1.48g of Reillex polymer containing ~ 2.24%Rh, assuming that all the rhodium incorporated uniformly during impregnation. Samples were tested by GC at 5,10, 20, 30, and 45 minutes, respectively. As starting materials, this run contained 145.65g acetic acid, 9.1g methyl iodide and 9.96g DME.

Experiment B
This catalytic run used 3.34g of Reillex polymer containing ~5.10%Rh, assuming that all the rhodium incorporated uniformly during impregnation. Samples were tested by GC at 5, 10, 20, 30, and 45 minutes, respectively. As starting materials, this run contained 144.28g acetic acid, 9.0g methyl iodide and 10.17g DME.

Experiment C
This catalytic run used 3.35g of Reillex polymer containing ~2.24%Rh, assuming that all the rhodium incorporated uniformly during impregnation. Samples were tested by GC at 5, 10, 20, 30, and 45 minutes, respectively. As starting materials, this run contained 146.20g acetic acid, 9.0g methyl iodide and 9.88g DME.

Experiment D
This experiment was a repeat of Experiment C with a fresh charge of acetic acid, methyl iodide, and DME.

Experiment E
This experiment was a repeat of Experiment D with a fresh charge of acetic acid, methyl iodide, and DME.

Experiment F
This catalytic run used 1.56g of Reillex polymer containing ~2.24%Rh that was treated with an equivalent of palladium acetate. Samples were tested by GC at 5, 10, 20, 30, and 45 minutes, respectively. As starting materials, this run contained 146.30g acetic acid, 9.0g methyl iodide and 10.53g DME.

To compare the results, mass balances were initially calculated by the formula {2[EDA] + [DME] + [MeOAc] + [acetic anhydride]} 100/Total [DME] added and expressed as %. The 2[EDA] is required because one EDA requires two DME for synthesis. Both MeOAc and acetic anhydride require one DME. With this formula the mass balances were found to worsen with time. Better mass balances were obtained by taking into account the ethyl acetate concentrations from the reduction of EDA and the methane concentration from the reduction of DME found by head-space analysis. To compare the various runs the following terms were defined:

Yield = {2[EDA]} 100/[DME] added
Conversion = {[MeOAc]reacted} 100/[DME added]
Selectivity = {2[EDA]} 100/[MeOAc] reacted
Conversion x Selectivity = Yield

The assumption in defining these expressions is that all the DME reacts cleanly with acetic acid to give methyl acetate. The results at 45 minutes are tabulated in Table 3.2.1.

Table 3.2.1 Dimethyl Ether to Ethylidene Diacetate Material Balance

EXP.	MASS BAL%	YIELD%	CONV%	SEL%
A	91.6	10.1	42.3	24
B	95.5	22.8	76.5	29.8
C	92.6	18.4	60	30
D	93.3	35.5	69.5	51
E	86.9	24.3	65	37.4
F	92.8	8.4	41.6	20

Comparison of Various Samples

Experiment A versus Experiment F

Both samples showed similar yields and selectivities at 45 minutes. The only difference between these two samples was that Experiment F was treated with $Pd(OAc)_2$. An elemental analysis of Experiment F sample after the run showed 1.73% Pd, which indicated that there is significant Pd concentration. The fact that there is very little difference in the catalytic activity of both samples indicates that it is the rhodium concentration that decides the activity.

Experiment A versus Experiment C

The only difference in both these samples is that approximately two times the catalyst was used in the Experiment C run. The yield of EDA at 45 minutes increased from 10% to 18.4%, which is to be expected.

Experiment C versus Experiment D versus Experiment E

These consecutive runs with the same catalyst showed that rhodium did not leach out significantly from run to run since the catalytic activity would be expected to diminish were this to occur. In fact, catalytic activity appeared to increase, and Experiment D and E runs had higher yields and selectivity towards the product EDA (see Table 3.2.1). The Rh analysis after Experiment E was found to be 1.73% compared to the theoretical of 2.2%. The 23% difference was probably not due to loss of Rh from the Reillex polymer, but rather to an increase in the molecular weight of polymer via methyl iodide incorporation. Additional supporting evidence was reported in the previous quarterly when the Rh concentration decreased from 2% to 1.63% after one run. Since the same decrease occurred even after three runs, this indicated that no additional catalyst was being leached out.

Experiment C versus Experiment B

Both of these runs had the same amount of Reillex, but a sample from Experiment B had a higher Rh concentration (5.1% versus 2.2%). However, no great increase in EDA yield was seen (22.8% versus 18.4%). In fact Experiment B produced more methane and less acetic anhydride than did Experiment C. It appears that a higher concentration of catalyst is detrimental, in that methane is produced by another mechanism. We plan to investigate this. Elemental analysis of Experiment B after the run showed a 3.93% Rh content compared to a 5.1% value. This 23% loss was similar to that observed with all samples. As discussed above, this is probably due to an increase in polymer weight from methyl iodide incorporation.

Background for Catalytic Runs (180 minutes, 300 cc autoclave)

The research effort focused on longer test times with rhodium / Reillux polymer for the catalytic conversion of DME to EDA. The goals were as follows:

- Perform a catalytic run for 180 minutes and compare the results with the 45 minute run from above.
- Repeat the catalytic run for 180 minutes using a fresh charge of reactants.

Catalytic Runs (180 minutes, 300 cc autoclave)

The catalytic run in Experiment G used ~1.5g of catalyst containing ~2.24% Rh by weight. Samples were analyzed by GC at 30, 60, 90, 120, 150 and 180 minutes, respectively. As starting materials, this run contained 144.7g acetic acid, 9.4g methyl iodide and 8.4g DME. A 1:1 ratio of CO/H_2 was used at a pressure of 1500 psi and a temperature of 190°C. A graphical representation of the concentrations of some products versus time is shown in Figure 3.2.1.

Figure 3.2.1 300cc Autoclave Run

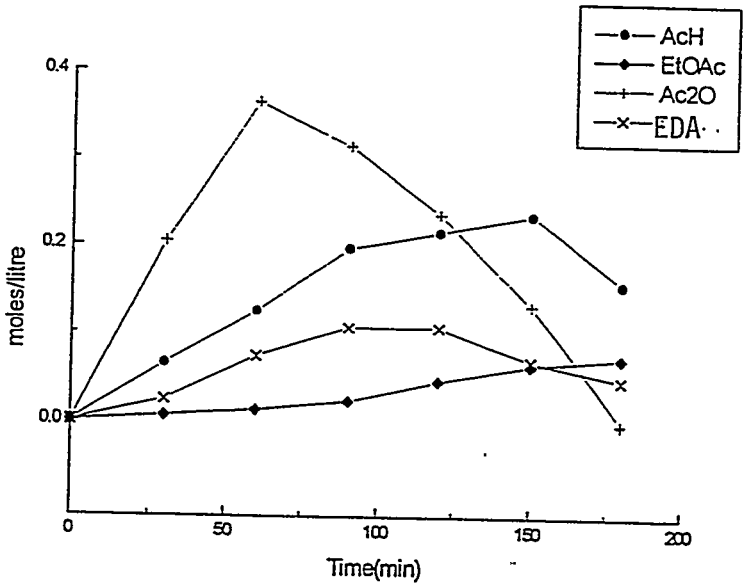

The graph shows that the EDA concentration continued to increase up to 90 minutes, after which it slowly decayed presumably by hydrogenation to give ethyl acetate and acetic acid. This reasoning is supported by the fact that the ethyl acetate concentration also began to increase after 90 minutes. The acetic anhydride concentration increased up to 60 minutes, after which it dropped rapidly. We have not yet characterized what the anhydride is converted to, but possibilities are acetic acid or acetone and carbon dioxide. The results also showed that the reaction between anhydride and acetaldehyde to give EDA was not rapid.

The catalytic run of Experiment H used the same catalyst as Experiment G with a fresh charge of starting materials. The results are shown in Figure 3.2.2.

Figure 3.2.2 300 cc Autoclave Run

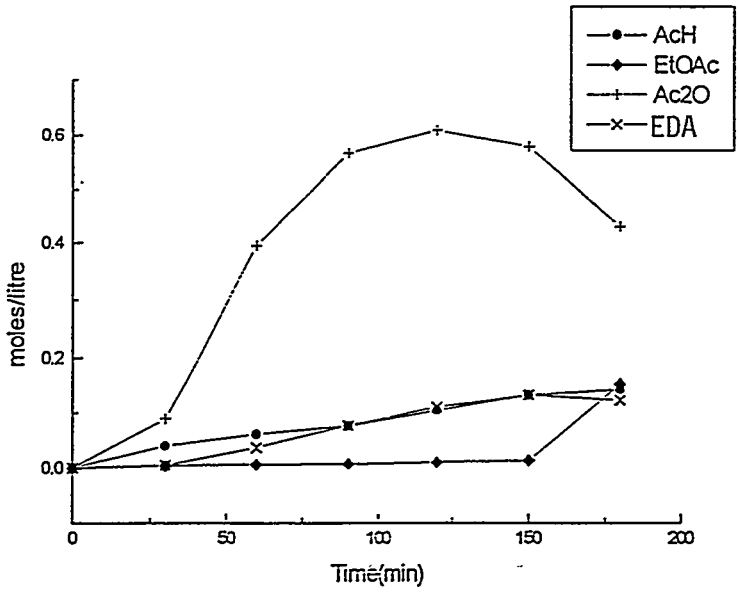

It can clearly be seen by a comparison with the results of Experiment G that the product distribution was different. The EDA concentration continued to rise slowly up to 150 minutes, after which it dropped slightly. The acetic anhydride increased to an appreciable concentration up to 150 minutes, after which it dropped steeply presumably via hydrogenation to give ethyl acetate, the concentration of which increased. It is interesting to note that both runs appeared to behave similarly up to 50 minutes. In order to numerically compare both the runs, the following equations are defined:

Yield = {2[EDA]} 100/[DME] added

Mass Balance = {2[EDA] + 2 [EtOAc] + [MeOAc] + [AcH] + [Ac2O] + [CH4]} 100/ {DME added]

Table 3.2.2 presents a comparison of yields and mass balances at various times during the reaction.

The mass balances in the Experiment G sample progressively worsened because the acetic anhydride was converted to other products not accounted for in the mass balance (see Figure 3.2.2). In contrast, the Experiment H sample had better mass balances because the acetic anhydride concentration was still appreciable at 180 minutes. It is also interesting to note that the yield of EDA at the 60 minute mark for Experiment G was 12.4%, which compares well with the 45 min. yield of 10.1% obtained with Experiment A in the first quarter report. The Experiment H sample showed only a 5.5% yield at 60 minutes, but with longer time the EDA concentration increased to 19.7%. This shows that after the 180 minute run, Exp G, the behavior of the catalyst has changed considerably from a fresh charge (Exp H). This result is different from that obtained for three consecutive runs (Exp C, Exp D, Exp E), when the yield of EDA at 45 minutes did not decrease. This indicates that the catalyst performs better for three 45 minutes runs than for a 180 minute run, implying that in a reactor, partial conversion with recycle is better than complete conversion.

Table 3.2.2 Dimethyl Ether to Ethylidene Diacetate Material Balance

EXP	TIME (min.)	EDA YIELD %	MASS BAL. %
G	30	4.0	88.7
G	60	12.4	90.8
G	90	17.9	78.7
G	120	17.9	68.8
G	150	11.5	55.1
G	180	8.0	42.6
H	30	0.7	82.8
H	60	5.5	87.2
H	90	11.4	90.3
H	120	16.4	87.7
H	150	19.7	85.1
H	180	18.4	93.2

Catalytic Runs (180 minutes, 100 cc autoclave)

We attempted to commission a smaller scale batch reactor (100cc) for the DME to EDA conversion. The first reaction tried was the homogeneously catalyzed reaction for which we already had successful results in a 300 cc reactor. However, the reaction did not progress as expected for three consecutive attempts. In all three cases the reactions were run for 3 hours with samples being taken every 30 minutes. The results from the first run are shown in Figure 3.2.3.

Figure 3.2.3 100cc Autoclave Run

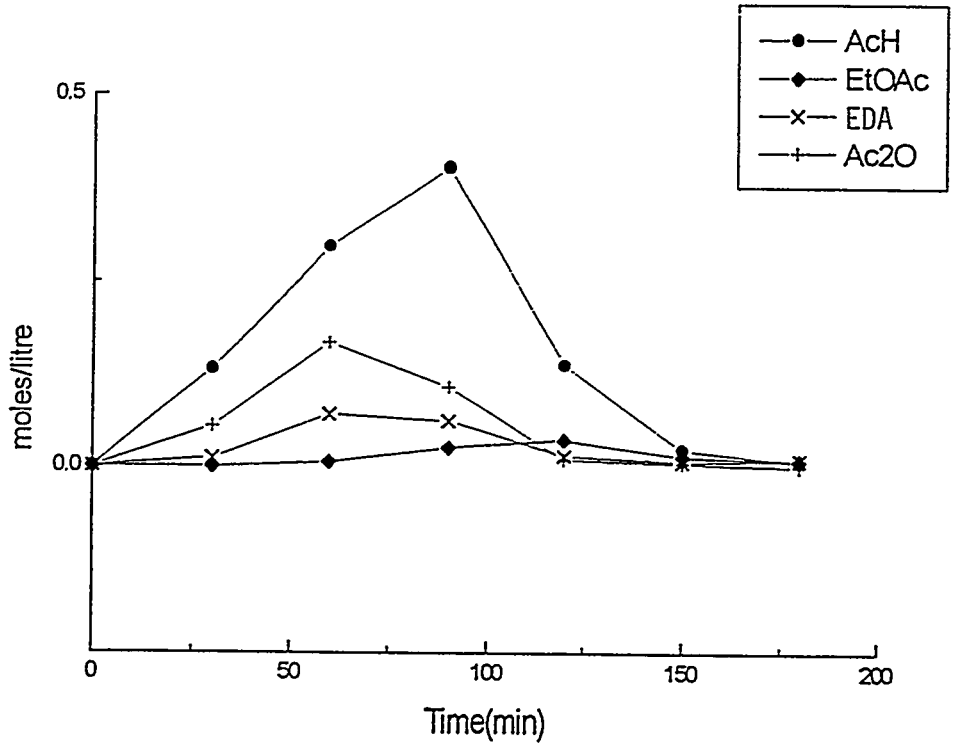

The graph shows that the major product until 90 minutes is acetaldehyde, after which it falls rapidly and is presumably converted to acetic acid. A low concentration of the desired product EDA is seen up to 60 minutes, after which it decays rapidly. However, no EDA was seen in the second and third runs (see Figure 3.2.4).

Figure 3.2.4 100 cc Autoclave Run

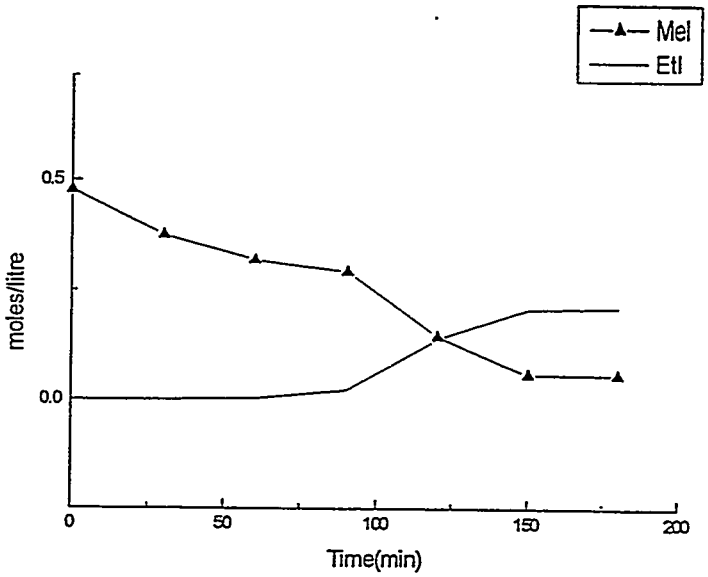

In all three runs the methyl iodide was converted to ethyl iodide (see Figure 3.2.5).

Figure 3.2.5 100 cc Autoclave Run